environmental microbiology

Environmental Microbiology (2022) **24**(4), 1946–1963 doi:10.1111/1462-2920.15951

Characterization of a *dszEABC* operon providing fast growth on dibenzothiophene and construction of broad-host-range biodesulfurization catalysts

Guadalupe Martín-Cabello, Laura Terrón-González and Eduardo Santero*

Centro Andaluz de Biología del Desarrollo, Universidad Pablo de Olavide/Consejo Superior de Investigaciones Científicas/Junta de Andalucía, and Departamento de Biología Molecular e Ingeniería Bioquímica, Universidad Pablo de Olavide, Spain.

Summary

A new operon for biodesulfurization (BDS) of dibenzothiophene and derivatives has been isolated from a metagenomic library made from oil-contaminated soil, by selecting growth of *E. coli* on DBT as the sulfur source. This operon is similar to a *dszEABC* operon also isolated by metagenomic functional screening but exhibited substantial differences: (i) the new fosmid provides much faster growth on DBT; (ii) associated *dszEABC* genes can be expressed without the need of heterologous expression from the vector promoter; and (iii) monooxygenases encoded in the fosmid cannot oxidize indole to produce indigo. We show how expression of the new *dszEABC* operon is regulated by the sulfur source, being induced under sulfur-limiting conditions. Its transcription is activated by DszR, a type IV activator of σ^N-dependent promoters. DszR is coded in a *dszHR* operon, whose transcription is in turn regulated by sulfur and presumably activated by the global regulator of sulfur metabolism CysB. Expression of *dszH* is essential for production of active DszR, although it is not involved in sulfur sensing or regulation. Two broad-host-range DBT biodesulfurization catalysts have been constructed and shown to provide DBT biodesulfurization capability to three *Pseudomonas* strains, displaying desirable characteristics for biocatalysts to be used in BDS processes.

Received 21 July, 2021; accepted 21 February, 2022. *For correspondence. E-mail esansan@upo.es.

Introduction

Sulfur is a natural component of crude oil, representing between 0.05% and 10% of its composition. Burning of fossil fuels releases sulfur dioxide, contributing greatly to acid rain, poisoning forests and lakes, corroding buildings and altering the natural balance of chemical elements in the environment, thus affecting ecosystems' biological diversity. Total particulate emissions, which are a serious source of air pollution, are directly proportional to the amount of sulfur in diesel fuel, 2% of the sulfur being converted into direct particulate emissions (Mohebali and Ball, 2016).

Environmental legislation, though highly variable among the countries, is in general increasingly restrictive, requiring the use of ultra-low sulfur level fuels in industrialized countries. In the petrochemical industry, sulfur removal is carried out mainly by hydrodesulfurization (Brunet *et al*., 2005). However, this is an expensive process that requires hydrogen, and high pressures and temperatures. In addition, many of the organic sulfur contaminants in fuel, such as dibenzothiophene (DBT), or its alkylated derivatives, are refractory to physicochemical desulfurization (Martinez *et al*., 2017; Wang *et al*., 2017).

Biodesulfurization (BDS), the biological removal of sulfur from organic molecules, is envisioned as a very attractive technology for sulfur removal from these fuel contaminants, refractory to hydrodesulfurization. BDS of S-heterocyclic compounds, such as DBT, is achieved by various microorganisms through different metabolic pathways, being the so-called 4S pathway, the most promising for developing BDS processes, as it removes sulfur from DBT without altering the rest of the molecule (Martinez *et al*., 2017). The pathway comprises four steps involving three monooxygenation reactions, the first two being catalysed by a sulfide-sulfoxide monooxygenase (DszC), and the third catalysed by a dibenzothiophene-5,5-dioxide monooxygenase (DszA). Once oxidized, sulfur is then hydrolyzed from the resulting molecule by a hydroxybiphenyl-2-sulfinate desulfinase (DszB), releasing bisulfite and 2-hydroxybiphenyl (2-HBP). The monooxygenation reactions require electrons that are provided

by an NAD(P)H/FMN-oxidoreductase (DszD) (Piddington *et al*., 1995; Gray *et al*., 1996).

Genes coding for the Dsz enzymes were first reported in *Rhodococcus erythropolis* strain IGTS8 (Denome *et al*., 1994) [currently *R. qingshengii* (Thompson *et al*., 2020)] and found to be closely located, even overlapping, in an operon designated *dszABC* (Piddington *et al*., 1995). Since then, well-conserved *dszABC* operons have been described in similar, compact arrangements in several replicons (plasmid or chromosome) of many Gram-positive and Gram-negative bacteria able to use DBT as the only sulfur source (reviewed in Martinez *et al*., 2017). It is frequent to find the *dszABC* operon linked to mobile DNA, which suggest that the operon might have been inserted laterally at different replicons through transposable elements (Denis-Larose *et al*., 1997; Ishii *et al*., 2000b). Importantly, *dszD* genes coding for the oxidoreductase, when identified, are shown to be unlinked from the structural *dszABC* operons, even located at different replicons (Ishii *et al*., 2000a; Furuya *et al*., 2004; Furuya *et al*., 2005).

Although regulation of *dsz* genes has not been well characterized, expression of these genes has been shown to be strongly repressed by preferred sulfur sources such as sulfate, cysteine, methionine or casaminoacids in Rhodococci (Li *et al*., 1996; Denis-Larose *et al*., 1997), *Mycobacterium* (Takada *et al*., 2005) and *Gordonia* (Alves *et al*., 2007; Feng *et al*., 2016). To date, only the *Gordonia* sp. IITR100 system has been characterized and shown to involve a TetR-family activator (Murarka *et al*., 2019; Murarka and Srivastava, 2019) and a global repressor, WhiB1 (Murarka *et al*., 2020). Both repressor and activator have been shown to bind at the *dsz* promoter region. Repression of *dsz* genes is mediated by preferred sulfur sources, and this repression requires sulfate assimilation (Tanaka *et al*., 2002). This would indicate that a global sulfur regulation mechanism, induced by sulfur limitation rather than a particular sulfur source, such as DBT, takes place in the activation/repression of *dsz* genes.

Sulfur regulation has been best characterized in Enterobacteria and in *Pseudomonas* (Kertesz, 2000). Both bacteria share a common master regulator, the LysR-type regulator CysB, which responds to sulfur availability by inducing the expression of genes involved in sulfur provision from non-preferred, alternative sulfur sources, such as taurine (*tau* genes) or aliphatic sulfonates (*ssu* genes). In *E. coli*, expression of *tau* and *ssu* genes requires a second regulator, Cbl (van der Ploeg *et al*., 2001), closely related to CysB. Cbl expression is activated by CysB, which may act in cascade at the *ssuEADCB* promoter (Stec *et al*., 2006), and in concert with CysB at the *tauABCD* promoter (van der Ploeg *et al*., 1997). No *cbl* gene has been detected in *Pseudomonas* genomes. Instead, a second regulator, SfnR, whose expression is activated by CysB in response to sulfur limitation (Endoh *et al*., 2003a), has been described to be involved in the expression of *sfn* genes required for utilization of dimethyl sulfide, dimethyl sulfone and dimethyl sulfoxide as sulfur sources (Endoh *et al*., 2003a; Endoh *et al*., 2003b; Endoh *et al*., 2005; Habe *et al*., 2007). A second copy of SfnR has been reported in *Pseudomonas aeruginosa*, being both SfnR1 and SfnR2 involved in dimethyl sulfide utilization (Habe *et al*., 2007; Lundgren *et al*., 2019), not acting as LysR-type regulators but as activators of σ^N-dependent promoters. Interestingly, SfnR proteins lack the N-terminal regulatory domain, which suggests these may act as constitutively active type IV activators (Bush and Dixon, 2012).

Despite the large number of bacterial strains able to grow on DBT as the only sulfur source isolated, and the attempts at manipulation to improve their functionality (Martinez *et al*., 2017; Parveen *et al*., 2020), an efficient BDS process to remove sulfur from fuels has yet to be industrially developed (Kilbane II, 2016; Martinez *et al*., 2017). One of the technical problems is that DBT biodegradation is repressed by other preferred sulfur sources, which has prompted to construct engineered strains expressing *dsz* genes from ectopic promoters (Gallardo *et al*., 1997; Takada *et al*., 2005; Alves *et al*., 2007; Khosravinia *et al*., 2018). In addition, other problems preclude development of biocatalysts, including substrate bioavailability, final product (2-HBP) toxicity, or enzyme product inhibition (Abin-Fuentes *et al*., 2013; Li *et al*., 2019). Therefore there is a need to pursue the search for new enzymes and novel bacterial strain characteristics to develop an efficient biocatalyst.

Since cultivated bacteria represent a very small fraction of the bacterial diversity (Vilchez-Vargas *et al*., 2010), thus providing an extremely limited view of the biodegradation potential available in nature, metagenomic analyses represent a potent approach to identify genes with novel characteristics, independently of the cultivation of the bacterium harbouring them. However, metagenomic studies have generally failed to identify functional *dsz* genes. One metagenomic sequence analysis reported the identification of a *dszABC* operon (Abbasian *et al*., 2016), although its functionality was not tested. More recently, a *dszEABC* operon, bearing all the genes required for DBT biodegradation, was identified by functional metagenomics and functionally characterized. In this case, the authors screened for the ability to oxygenate indole to produce the blue pigment indigo (Martin-Cabello *et al*., 2020). Now, we report on the isolation of a new fosmid able to sustain very fast growth on DBT as the only sulfur source to the surrogate *E. coli* strain hosting it. The fosmid bears all the biodegradation genes

clustered in a single operon. Expression of the *dsz* operon in this fosmid has been characterized and shown to be repressed by sulfate. These genes have been cloned into broad-host-range vectors and shown to work efficiently on a number of *Pseudomonas* strains with different characteristics relevant for developing efficient BDS processes.

Results

Isolation of a fosmid providing ability to grow on DBT as the sulfur source

A 6.5 Gb of DNA metagenomic library from an oil-contaminated soil (Terron-Gonzalez *et al*., 2016) was used as a donor in triparental matings in order to detect DBT BDS genes. The recipient was a nalidixic-resistant derivative of the specialized *E. coli* strain MPO554, able to increase the fosmid copy number with arabinose and to transcribe the environmental DNA from a *Psal* promoter present in the vector, being this transcription subjected to antitermination by the lambda phage N protein (Terron-Gonzalez *et al*., 2013). To increase fosmids copy number, mating mixtures were plated in minimal medium containing arabinose, salicylate (to induce transcription from the vector *Psal* promoter) and DBT (as the only sulfur source).

Fast-growing transconjugants appeared before 48 h of growth with a frequency of 10^{-6} per recipient cell, together with several slower-growing transconjugants that appeared days later. Following confirmation of fast growth on DBT of many transconjugants, DNA from 20 of them was isolated and shown to carry a fosmid with the same restriction pattern. One transconjugant bearing the fosmid designated UPO112 was selected for further characterization.

We tested MPO554Nal^r/UPO112 for dependence on arabinose or salicylate for growth on DBT (Fig. 1) and showed much faster growth and higher final cell density than those carrying the DBT biodegradation fosmid UPO21, previously isolated from the same metagenomic library (Martin-Cabello *et al*., 2020). Unlike UPO21, growth on DBT conferred by UPO112 was entirely independent of salicylate or arabinose; in fact, poorer growth was observed with their addition. Therefore, genes coding for DBT biodegradation in UPO112 can be expressed to sufficiently high levels to support fast growth of *E. coli* on DBT without further induction. Furthermore, while the UPO21 fosmid had been isolated by a functional screen for the indigo production on Lysogeny Broth (LB) plates, UPO112 did not provide this capability (Supplementary Fig. S1), suggesting that the DBT biodegradation genes present in UPO112 are different from those in UPO21.

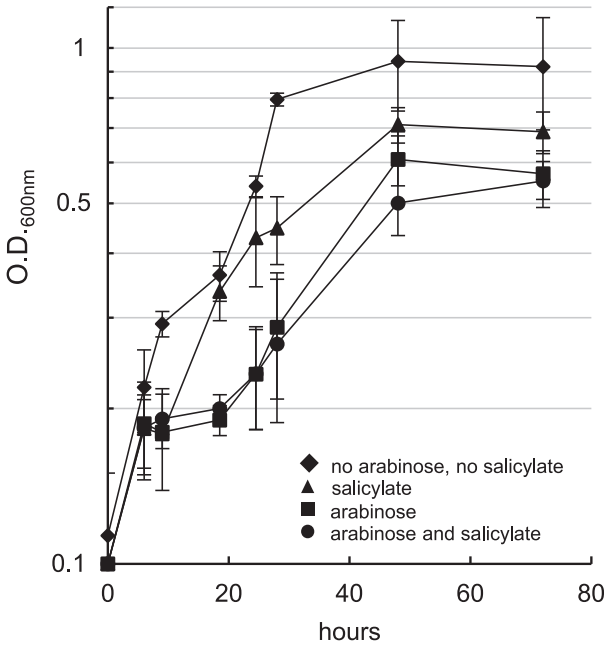

Fig. 1. Growth of MPO554/UPO112 in minimal medium M9 with 0.2 mM DBT as the only sulfur source. Values are the average of at least three independent replicates; error bars represent standard errors. Residual growth up to O.D.600 = 0.2 due to sulfur previously accumulated by the cells was observed in the control strain bearing the empty vector pMPO579, but it is not shown for clarity.

The efficiency of DBT use, or even the more recalcitrant dimethylated derivative 4,6-dimethyl dibenzothiophene (4,6-DMDBT) as the sulfur source was tested and compared to growth when using the sulfur-sufficient source sulfate, or taurine (2-aminoethanesulfonic acid), a sulfur source for *E. coli*, whose utilization is repressed by sulfate (Sekowska *et al*., 2000; van der Ploeg *et al*., 2001). As shown in Fig. 2, sulfate was the best sulfur source, closely followed by taurine. However, the culture was also able to grow efficiently on DBT, reaching the stationary phase within 26 h. After full growth, supernatants of the 0.2 mM DBT cultures accumulated 0.18 mM 2-HBP as the final product, thus showing an almost stoichiometric relationship between the substrate and the product, and confirming DBT utilization via the 4S pathway. Finally, although 4,6-DMDBT was clearly the poorest sulfur source, the genes within UPO112 also supported growth on this recalcitrant compound, thus making these genes promising candidates for development of efficient BDS biocatalysts.

Sequence analysis of genes comprised in UPO112

The fosmid UPO112 was fully sequenced and shown to harbour an insert of 36 281 bp potentially coding for 36 complete *orfs* (Fig. 3A). Genes coding for products involved in BDS of DBT were found in this fosmid, which

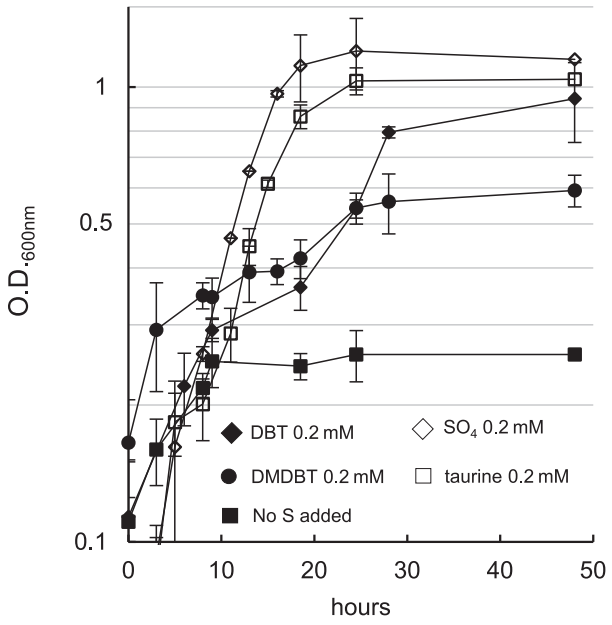

Fig. 2. Growth of MPO554/UPO112 in minimal medium M9 with different sulfur sources. Growth curves with DBT or DMDBT started at O.D.600 = 0.1, whilst growth curves with taurine or sulfate started at O.D.600 = 0.05 in order to do all the experiments at the same time. Values are the average of at least three independent replicates; error bars represent standard errors.

showed very high levels of identity with those previously identified in UPO21 (more than 71% of aa identity; Fig. 3B). Phylogenetic trees of DszABC gene products shown in supporting Fig. S2 indicate that Dsz proteins coded in the fosmids conform distinctive branches separated from other Dsz gene products but still more closely related to Dsz proteins than to Bds or Tds proteins. The four conserved motives found in DszA and DszB and the two conserved regions found in DszC (Kilbane 2nd and Robbins, 2007) are also present in the Dsz proteins coded by fosmids sequences. Interestingly, the Phenylalanine residue in region 1 of DszB, which is not conserved in two *Gordonia* encoded products, is neither conserved in DszB from UPO112, all containing a Tyrosine instead. As in fosmid UPO21, a fourth gene designated *dszE*, coding for an FMN oxidoreductase similar to oxidoreductases involved in aliphatic sulfonates BDS (Fig. 3C), preceded the *dszABC* genes. Interestingly, *dszE* from UPO112 was highly similar to a gene encoded in the recently sequenced genome of *Comamonadaceae bacterium* (MBH2042284.1. Accession number of the scaffold: JAECRK010000006.1). This gene preceded other three genes similar to *dszABC* (MBH2042285.1, MBH2042286.1 and MBH2042287.1), although they were not annotated as such in the genome sequence. As in most operons described in biodesulfurizing strains, including UPO21, *dszABC* genes overlap, and the *dszE* gene is positioned in close proximity to *dszA* (separated by just 5 bp), thus forming a very compact *dszEABC* operon likely to be translationally coupled (Fig. 3A).

Besides the four *dsz* genes directly involved in DBT desulfurization, six adjacent *orfs* showed high similarity to *orfs* present in UPO21. These include the previously identified regulatory gene *dszR*, coding for a σ^N-dependent activator protein, the four *orfs* separating the regulatory and structural *dsz* genes, which encode for products with different unrelated functions, and a gene upstream *dszR* that encodes for a product with unpredicted function, which has been designated *dszH* (see below). The degree of similarity of these *orfs* to those in UPO21 was substantially lower than that of the Dsz products, their percentage of identity ranging from 38% to 69% (Fig. 3B).

As previously described for UPO21 (Martin-Cabello *et al*., 2020), phylogenetic analyses of UPO112 *orfs* showed two potential evolutionary origins, the *dszABC* genes likely arising in Actinobacteria while the remaining, and including *dszE* and *dszHR*, originating in Proteobacteria.

Sequences flanking these homologous regions in both fosmids were completely unrelated, suggesting that the conserved genes constitute a genomic island that might have been transferred laterally to different genomes. Several truncated and complete *orfs*, potentially coding for transposases/integrases, were identified immediately upstream of *dszE* in UPO112 (Supporting Table S1), while being absent in UPO21. This putative genomic island is slightly larger in UPO112 than in UPO21 (10 278 bp vs. 9502 bp respectively), mainly due to an increased intergenic distance between *dszR* and *dszE*. Interestingly, the intervening DNA that separates *dszR* from the gene upstream in UPO21 is absent in UPO112, thus conforming a *dszHR* operon, translationally coupled presumably, with overlapping stop and start codons (ATGA).

Orfs flanking the putative genomic island in UPO112 display highest similarity to *orfs* of the recently sequenced genome of *Candidatus* Macondimonas diazotrophica (BLAST analyses, Supporting Table S1), a nitrogen-fixing oil degrader *γ-Proteobacteria* abundant in crude-oil contaminated coastal sediments (Karthikeyan *et al*., 2019). In many instances, flanking *orfs* in the fosmid share the same arrangement observed in the Macondimonas genome, although some rearrangements have taken place (Supplementary Table S1). Flanking *orfs* in UPO21 were also analysed, revealing that the *dsz* genes in UPO21 probably come from a genome similar to that of *Candidatus* Macondimonas diazotrophica (Supplementary Table S2), although the putative genomic island is located in a genomic context different from that of UPO112. Interestingly, the published *Candidatus*

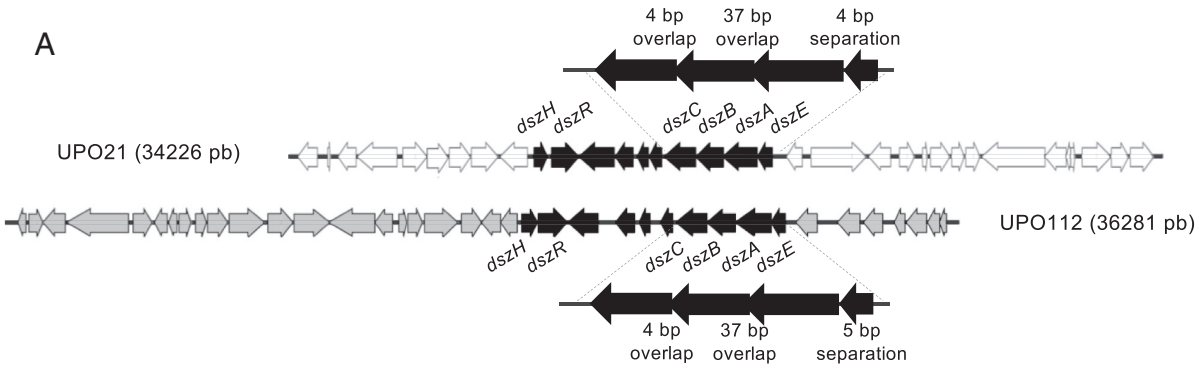

B

UPO112	UPO21	Coverage	Identity
DszH	DszH	92 %	38 %
DszR	DszR	100 %	72 %
Orf24	Orf13	82 %	68 %
Orf25	Orf14	98 %	69 %
Orf26	Orf15	100 %	58 %
Orf27	Orf16	94 %	70 %
DszC	DszC	100 %	91 %
DszB	DszB	100 %	82 %
DszA	DszA	100 %	90 %
DszE	DszE	100 %	72 %

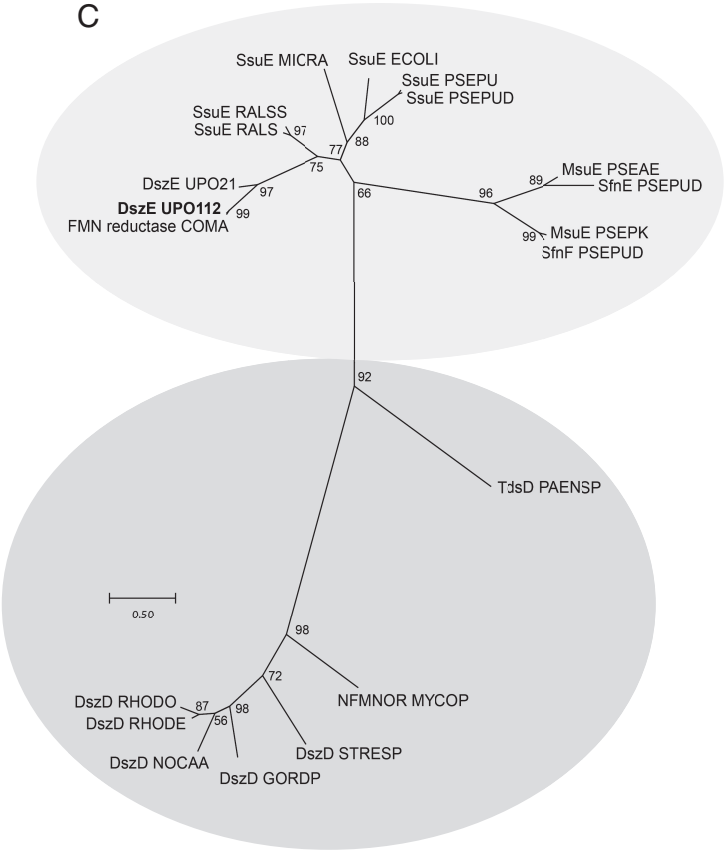

Fig. 3. A. Schematic diagram comparing UPO21 and UPO112 clones. Putative orfs and their orientations are shown. Conserved genes included in the genomic island, containing genes involved in dibenzothiophene desulfurization or not, are coloured in black.
B. Identity and coverage between UPO112 and UPO21 gene products coded by the genomic island.
C. Phylogenetic tree with DszE from UPO112 and UPO21 and other oxidoreductases. The scale indicates the amino acid substitutions per position. The GenBank accession numbers of oxidoreductases included in the phylogenetic tree are as follows: SsuE5_RALS: FMN reductase (NADPH), Ralstonia (WP_045787849.1); SsuE_MICRA: FMN reductase (NADPH), *Microcystis aeruginosa* (WP_012265981.1); SsuE_PSEPU: FMN reductase (NADPH), *Pseudomonas putida* (O85762.2); SsuE_ECOLI: FMN reductase (NADPH), *Escherichia coli* K-12 (P80644.2); MsuE_PSEAE: FMN reductase (NADPH), *Pseudomonas aeruginosa* PAO1 (O31038.1); MsuE_PSEPK: FMN reductase (NADPH), *Pseudomonas putida* KT2440 (Q88J85.1); SsuE_RALSS: FMN reductase (NADPH), *Ralstonia solanacearum* (WP_039549499.1); DszD_STRESP: NADH-dependent FMN reductase DszD, *Streptomyces* sp. NBRC 110027 (GAO11166.1); DszD_RHODE: DszD, *Rhodococcus erythropolis* (ABV44406.1); DszD_RHODO: NADH-dependent FMN reductase DszD, *Rhodococcus opacus* B4 (BAH52549.1); DszD_GORDP: NADH-dependent FMN reductase DszD, *Gordonia polyisoprenivorans* (GAB24076.1); DszD_NOCAA: NADH-dependent FMN reductase DszD, *Nocardia asteroides* NBRC 15531 (GAD84696.1); TdsD_PAENSP: thermophilic NAD(P)H-flavin oxidoreductase, *Paenibacillus* sp. A11-2 (BAB13707.1); Frm_MYCOP: NADH-FMN oxidoreductase, *Mycolicibacterium phlei* (BAD83685.1); SfnE_PSEPUD: NADH-dependent FMN reductase, *Pseudomonas putida* DS1 (Q845S9.1); SsuE_PSEPUD: NADPH-dependent FMN reductase, *Pseudomonas putida* DS1 (BAC00971.1); SfnF_PSEPUD: NADH-dependent FMN reductase, *Pseudomonas putida* DS1 (BAD51729.1); FMN_reductase_COMA: NADPH-dependent FMN reductase, Comamonadaceae bacterium (MBH2042284.1).

Macondimonas diazotrophica genome does not seem to contain *dsz* genes.

Sulfur starvation-induced expression of dsz *genes*

Unlike UPO21, *dsz* genes in UPO112 were expressed from their own promoter. In order to establish whether this expression was constitutive or regulated, a transcriptional *dszE*$_{UPO112}$*::lacZ* transcriptional fusion was constructed and then transferred to MPO554NalR carrying UPO112.

As shown in Fig. 4, *dszE* expression was low under sulfate growth conditions, and significantly induced (15-fold) when using DBT as the only sulfur source. Induction was moderately higher (18-fold) when using taurine. Taurine and DBT did not act synergistically. Induction was strictly dependent on the presence of the *dszE* promoter, since a control strain, carrying only the empty fusion vector, displayed basal expression levels independently of growth conditions. Addition of sulfate in presence of taurine or DBT abolished expression, which indicates that the *dszEABC* operon of UPO112 is repressed by sulfate rather than induced in response to a particular substrate such as DBT. On the other hand, in medium lacking all sulfur sources, which could not support growth, the *dszEABC* operon was not expressed, thus suggesting that efficient expression of this operon requires sulfur-limitation but also growth.

The UPO112 fosmid also bears the *dszR* regulatory gene, previously identified in the UPO21 fosmid as a σ^N-dependent transcriptional activator required for transcription from the *dszE* promoter (Martin-Cabello *et al*., 2020). Alignment of the *dszE* upstream regions in both fosmids also identified regions of very high similarity in the Shine–Dalgarno sequence, and also in the further upstream σ^N-dependent promoter sequence and in the palindromic sequences identified in UPO21 as the DszR binding sites (Fig. 5), thus suggesting that transcriptional control of both operons was similar and required DszR. To confirm this and to analyse the expression of the putative regulatory *dszR* gene, mRNA levels for each coding gene were quantified by RT-qPCR analysis in MPO554Nal^r/UPO112 growing under different sulfur sources. As shown in Fig. 6A, expression of *dszE* was highly induced when growing in taurine (49-fold), and even higher when growing in DBT (100-fold). As expected for a regulatory gene, transcription levels of *dszR* were much lower than those of *dszE*, although it also showed a consistent, though modest, increase (fivefold) when growing on the sulfur-limiting sources (Fig. 6B).

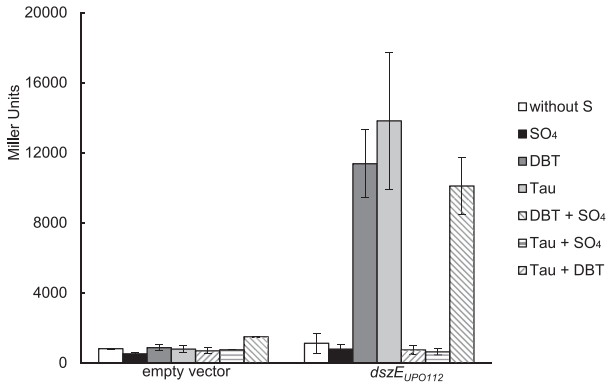

Fig. 4. Expression levels of *dszE*$_{UPO112}$*::lacZ* transcriptional fusion (pMPO1550) or the empty fusion vector (pMPO234), in MPO554/UPO112, in minimal medium M9 with different sulfur sources. Values are the average of at least three independent replicates; error bars represent standard errors.

dszEABC expression requires dszHR

To confirm that *dszR* is involved in the regulation of the *dszEABC* operon expression, the gene was subcloned. Since *dszR* was preceded by the *dszH* gene, both genes are part of the same operon and presumably are translationally coupled, the complete *dszHR* operon and 224 bp upstream of the *dszH* initiation codon was subcloned into the same fosmid vector backbone to generate pMPO1552, which was introduced into the MPO554Nal^r strain together with the plasmid bearing the *dszE::lacZ* transcriptional fusion; *dszE* expression was tested on sulfate or taurine growth media. As shown in Fig. 7A, *dszE* expression was low on sulfate but increased 28-fold on taurine, thus reproducing the sulfate repression observed with the full UPO112 fosmid, which indicates that the functional *dszHR* promoter is within the subcloned region.

To confirm that *dszE* induction was specifically responding to sulfur limitation and not to a general nutrient limitation, *dszE* expression was also tested when growing on the conventional nitrogen-sufficient source ammonium or the nitrogen-limiting sources glutamine or arginine, under sulfur-sufficient or sulfur-limiting conditions. Although nitrogen limitation modestly increased *dszE* expression under sulfur-sufficient conditions (fourfold to fivefold), this effect was smaller than that produced by sulfur limitation. Under sulfur-limiting conditions, nitrogen limitation had a very subtle effect (Fig. 7B).

To study the potential implication of *dszH* in the expression of the *dszEABC* operon under sulfur-limiting conditions, a derivative of pMPO1552, carrying an internal in frame deletion of 188 codons of *dszH* was constructed (Δ*dszH*-1; fosmid pMPO1561). The new fosmid was introduced into the MPO554Nal strain together with the plasmid bearing the *dszE::lacZ* transcriptional fusion, and *dszE* expression was tested on sulfate or taurine growth media. As shown in Fig. 7C, induction of the

```
UPO21   TCCCTTTTGGCTGCGCGCCAGGCAGCAGGGCTTGGCCCGGTTTGCGGCGCTGGCAGCACC
UPO112  CCTTACCGCCCTGCTGAATACTCAGCAGAAATCGGGCTCGCCTGCGGCTCACGCAGCAGC
         *          ****      *  ******    * ** *  *  ******  *  ******  *
UPO21   GCGGTTCGGCTGAAAAGCGCATTAACCATTCAAATACAGTGTGTTGAATCCTGGCATGAC
UPO112  GGATTAAAAACGACCGATAAATTCCCAAATAAAACAA--CTAGATATAAATTGGCATAAG
        *   *       **         ***  * * * *** *       * *  *   ****** *
UPO21   CTCTGCTTTATGCATATTGGATCTGAAAAATCCAGTTGTTCA--TAAGGAAACGTCATGG
UPO112  AAATGCTTTTTAGGCTGTGTCTTTGCATATACAGCTCTTAAATAAAAGGAAGTGCTATGC
           ****** *       **  * ** * *  *   *  * *  *   ******  *  ***
```

Fig. 5. Alignment of $dszE_{UPO21}$ and $dszE_{UPO112}$ upstream regions. Palindromic DszR binding sites are boxed; σ^N-dependent promoters are marked in light grey; arrow indicates the transcription start point experimentally mapped for UPO21 (Martin-Cabello *et al*., 2020); Shine–Dalgarno sequences in bold and start codon marked in dark grey.

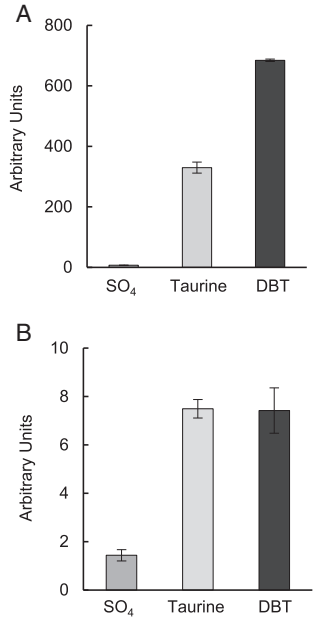

Fig. 6. Transcriptional levels of $dszE_{UPO112}$ (A) and $dszR_{UPO112}$ (B) measured by RT-qPCR assay, with cDNA retrotranscribed from RNA obtained from MPO554/UPO112 grown in minimal medium M9 with different sulfur source. Values are the average of at least three independent replicates; error bars represent standard errors.

dszEABC operon was completely abolished, thus indicating that *dszH* is required for *dsz* operon expression.

To complement the Δ*dszH*-1 mutation, the *dszH* gene without its own promoter was subcloned under the control of the P_{tac} promoter into the pMPO1571 vector, and introduced into the strain MPO554Nal^R, carrying pMPO1550 (*dszE::lacZ*) and pMPO1561 ($dsz\Delta H_1R$). However, as shown in Fig. 7D providing *dszH in trans* did not increase expression levels, thus suggesting that it is not the DszH protein itself but the coexpression of *dszHR* what is needed for effective production of an active DszR.

As expected for an in frame deletion, RT-qPCR analysis of *dszR* expression showed that transcription of the activator gene was only slightly reduced by the *dszH* deletion (Fig. 7E), which suggests that limitation of DszR-mediated activation due to the absence of *dszH* should reside in a step after *dszR* transcription.

Regulated expression of dszEABC when dszHR is ectopically transcribed

As the regulatory *dszHR* operon was itself regulated by sulfur limitation, one possibility is that regulation of the structural *dsz* operon relied on the transcriptional control of the *dszHR* operon rather than on the control of the DszR regulatory activity in response sulfur limitation. To establish the nature of the response to sulfur limitation, the regulatory operon devoid of its own sulfur-responsive promoter region was cloned immediately downstream of the IPTG-inducible P*tac* promoter in the expression vector pIZ1016 to yield pMPO1559. A version of this plasmid bearing a different internal in frame Δ*dszH* of 177 codons, (Δ*dszH*-2) was also constructed to generate plasmid pMPO1563-H.

As shown in Fig. 8, basal expression of *dszHR* in the absence of IPTG was sufficient to induce *dszE::lacZ* at high levels independently of the sulfur source. However, the Δ*dszH*-2 in frame deletion reduced considerably the expression levels of *dszE::lacZ* under all conditions, consistent with a *dszH* requirement for *dszEABC* expression. Upon induction of *dszHR* by IPTG, growth of the strains was slightly slower, which presumably limited *dszE* expression, while also displaying high *dszE* expression levels irrespective of the sulfur source. However, when $dsz\Delta H_2R$ is overexpressed, the *dszH* deletion had no effect on the induced expression levels of *dszE*. These data indicate that DszR can activate *dszEABC* transcription regardless of the sulfur source when ectopically transcribed from a P_{tac} promoter, with *dszH* somehow required. In addition, also shows that *dszH* is no longer required in the presence of high levels of DszR.

Toxicity of 2-HBP in E. coli *and* Pseudomonas

One of the main limitations of DBT biodegradation efficiency via the 4S pathway is the concomitant production of 2-HBP, which has been shown to inhibit growth and DBT biodegradation itself (Abin-Fuentes *et al*., 2013; Li *et al*., 2019). To test how 2-HBP accumulation could affect *E. coli* growth, a specialized strain bearing the UPO112 fosmid was grown in minimal medium with the

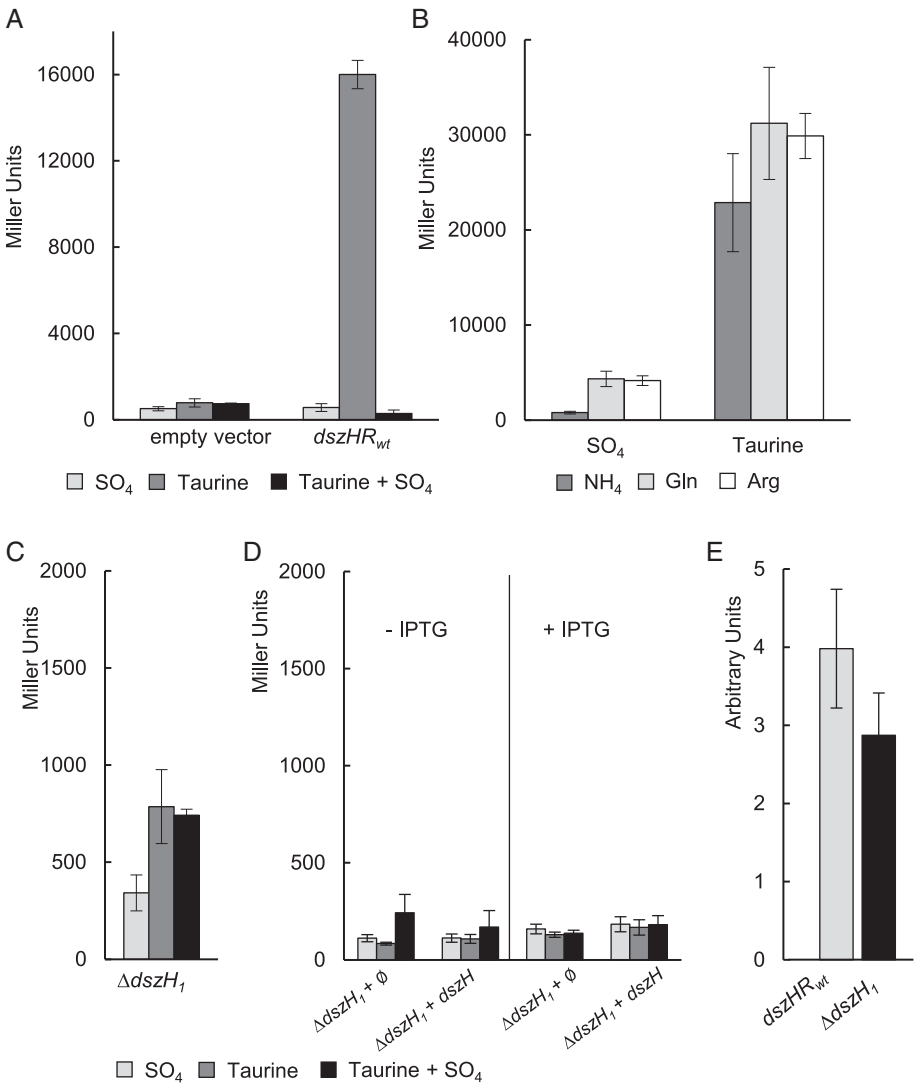

Fig. 7. Expression levels of *dszEUPO112::lacZ* transcriptional fusion (pMPO1550) in different sulfur or nitrogen sources in strains bearing the subclones pMPO1552 (*dszHR*$_{wt}$ from P$_{sal}$ promoter)(A) and (B)), pMPO1561 (ΔdszH) (C), or pMPO1561 also complemented in trans with pMPO1571 (*dszH*$_{wt}$ expressed under P$_{tac}$ promoter, induced or not with IPTG (D). Transcriptional levels of *dszR* measured by RT-qPCR assay, of the strains bearing/pMPO1552 or pMPO1561 grown in minimal medium M9 with taurine are also shown in (E). In all the panels, values are the average of at least three independent replicates; error bars represent standard errors.

different sulfur sources, and the effect on growth of increasing concentrations of 2-HBP was tested.

As shown in Fig. 9A, addition of 0.2 mM 2-HBP had little effect on bacterial growth, independently of the sulfur source. However, higher 2-HBP concentrations affected growth parameters. The magnitude of the effect was similar regardless of the sulfur source (Table 1), which indicated that bacterial growth limitation was due to general toxicity of 2-HBP rather than inhibition of DBT biodegradation activities.

To compare its tolerance to 2-HBP relative to other bacteria frequently used for contaminant biodegradation, such as *Pseudomonas*, we performed a tolerance test using serial dilutions on *E. coli* bearing the fosmid, and the KT2440 and DOT-T1E strains of *Pseudomonas*. As shown in Fig. 9B, although *E. coli* was quite tolerant to 0.2 mM 2-HBP, the *E. coli* strain was clearly more sensitive than any of the *Pseudomonas* strains, which tolerated 0.6 mM of exogenous 2-HBP.

Construction of DBT biodesulfurization broad-host-range vectors

To easily transfer the DBT BDS capacity among Gram-negative bacteria, which might be more efficient biocatalysts for DBT removal, the *dszEABC* operon and the regulatory *dszHR* genes were cloned into the broad-host-range vector pSEVA221 and introduced into KT2440 and the solvent-tolerant DOT-T1E strain. As shown in Fig. 10A, both strains carrying the catabolic genes were able to grow on DBT as the only sulfur source, thus indicating that the *dsz* genes could also be expressed in these strains. Cultures from both strains

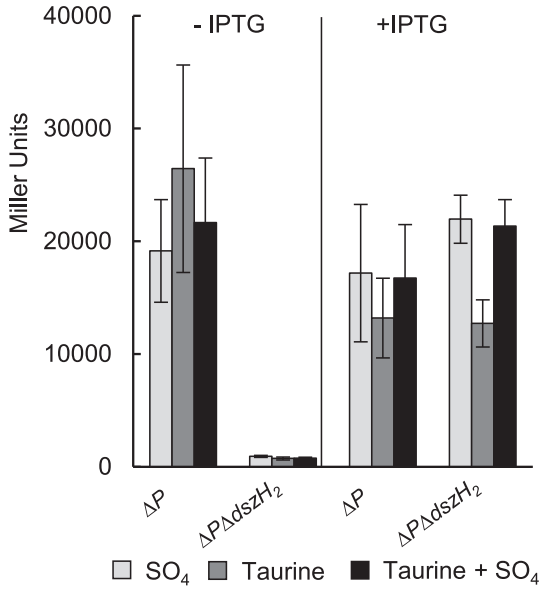

Fig. 8. Expression levels of *dszEUPO112::lacZ* transcriptional fusion (pMPO1550) in the plasmid ΔP_{dszHR} (pMPO1559) or the plasmid ΔP_{dszHR} $\Delta dszH_2$ (pMPO1563), both of them from P_{tac} promoter in minimal medium M9 with different sulfur source, without addition of IPTG (left panel) or with addition of IPTG (right panel). Values are the average of at least three independent replicates; error bars represent standard errors.

grown on DBT accumulated 2-HBP after growth (Table 2). However, 2-HBP was not detected in sulfate plus DBT cultures, which suggests that the DBT biodegradation capacity is also repressed by the preferred sulfur source in the *Pseudomonas* strains.

To prevent sulfate repression and improve the performance of these bacterial biocatalysts, the *dszEABC* operon was also cloned into pSEVA429, downstream of the P_{alkB} promoter, thus being able to induce transcription by alkanes (Silva-Rocha *et al*., 2013). This plasmid was introduced into the mentioned *Pseudomonas* strains, and also into MPO406, a KT2440 mutant derivative shown to hyperproduce biofilms (Amador *et al*., 2010; Amador *et al*., 2016), as this constitutes a characteristic of interest in DBT biodegradation biocatalyst development (Dorado-Morales *et al*., 2021).

As shown in Fig. 10B, all strains were able to grow on DBT as the only sulfur source. In the case of MPO406, growth on DBT was also detected in the absence of the inducer dicyclopropylketone (DCPK), but improved in its presence. Intriguingly, this was not the case for KT2440 or DOT-T1 strains, in which growth was increased further in the absence of the inducer, suggesting that basal expression levels of the *dsz* from the *PalkB* promoter were enough to support growth. As before, growth on DBT resulted in a concomitant 2-HBP accumulation in the culture medium (Table 2). Furthermore, production of 2-HBP in the presence of DBT plus sulfate decreased threefold to fourfold (Table 2), probably due to the faster growth conditions that precluded the elimination of all DBT before reaching the stationary phase. DCPK is known to exhibit a degree of toxicity, also observed in cultures that use sulfate as the sulfur source. This toxicity, which is less evident in the MPO406 biofilm hyperproducer strain (not shown), might explain the slower growth of KT2440 and DOT-T1 strains in the presence of DCPK.

Discussion

To identify genes encoding for the whole DBT BDS pathway, we performed a new functional screening in a metagenomic library by directly applying selection for growth on DBT as the only sulfur source. The 20 positive hits selected for further characterization were shown to harbour the same fosmid: UPO112. We know this is not the only fosmid in the library able to confer growth capacity on DBT, as fosmid UPO21, previously isolated from the same metagenomic library by a phenotype-change screening (Martin-Cabello *et al*., 2020), was not identified in the current screening. The selection procedure was designed to identify fosmids able to ensure very fast growth on DBT (visible colonies in less than 48 h), thus being blind to less efficient, such as UPO21. In fact, more colonies appeared in the selective medium after longer incubation times, although these were not characterized. Importantly, the growth rate on DBT as the sulfur source of *E. coli* carrying UPO112 is comparable to the most efficient strains previously reported, or even higher.

Curiously, UPO112 did not change the colour of the colony, unlike UPO21, which may explain why it was not identified in a previous screening (Martin-Cabello *et al*., 2020). This, together with its better performance, indicated that the genes in UPO112 were different from those in UPO21, and in turn highlights the importance of using multiple functional screening approaches to increase hit diversity.

Sequencing UPO112 revealed the existence of an operon encoding for the *dszEABC* genes required for DBT biodegradation, which are very similar to those previously reported for UPO21, and with the same genetic arrangement within a tightly packed operon. The *dszA* and *dszB* genes in these fosmids showed a longer overlap (37 bp) than the usual 4 bp overlap seen in other operons from various species. Since the 4 bp overlap seems to diminish expression of *dszB* (Li *et al*., 2007), a more extensive overlap might improve translational coupling between these genes. Longer overlaps have also been reported in *Gordonia alkanivorans* strains (Shavandi *et al*., 2010), though not in *G. amicalis* (Kilbane 2nd and Robbins, 2007). Similarly, the 4–5 bp gap between *dszB* and *dszC* is shorter than the 10–

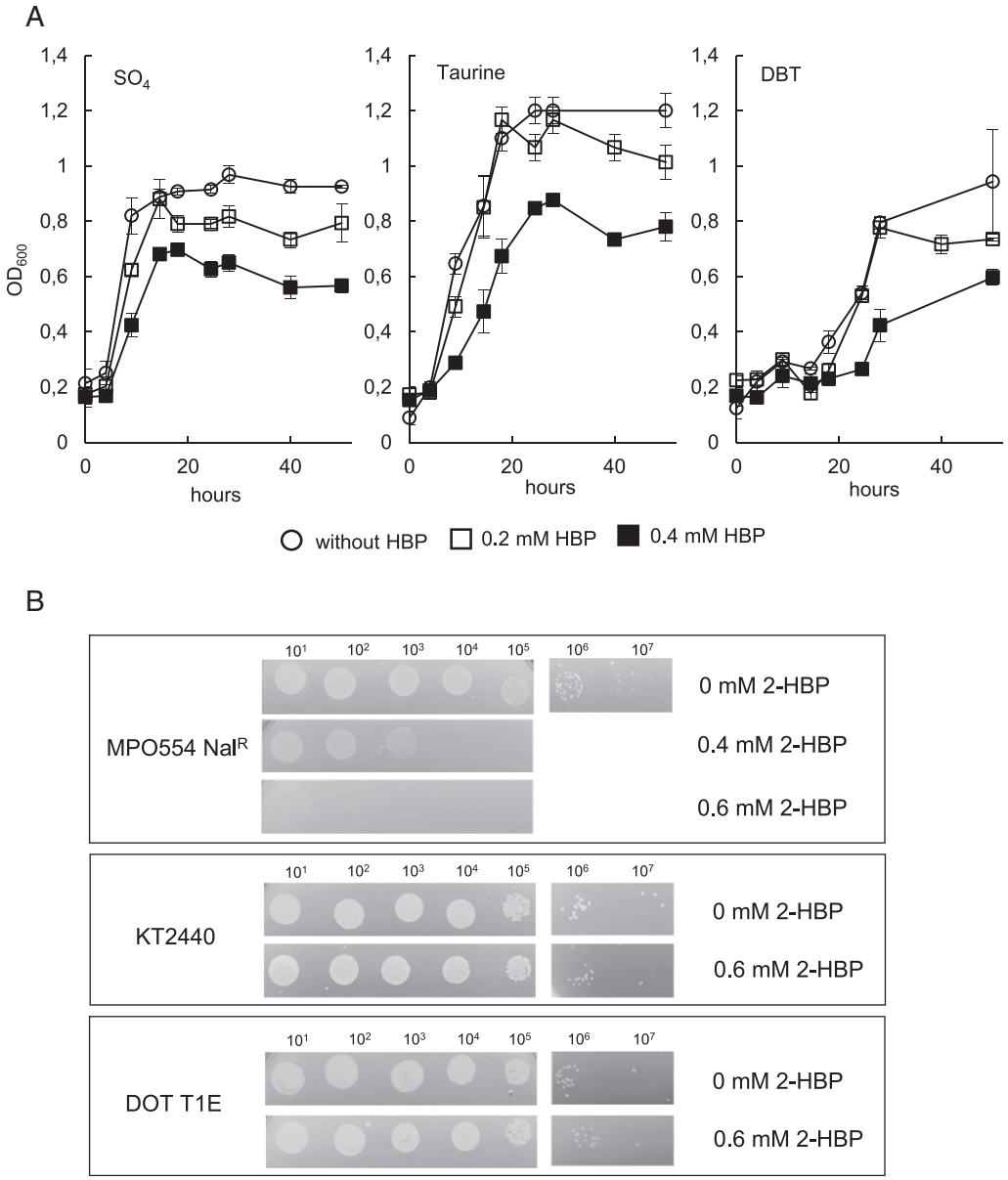

Fig. 9. A. Growth of MPO554/UPO112 in minimal medium M9 with different sulfur sources, with addition of 2-HBP (0.2 mM empty squares or 0.4 mM circles) or without 2-HBP addition (filled squares). Values are the average of at least three independent replicates; error bars represent standard errors.
B. Drop dilution assay to evaluate the sensitivity of *E. coli* MPO554 NalR, *P. putida* KT2440 and DOT T1E to 2-HBP. In minimal medium with sulfate and 0.4 mM (left panels) or 0.6 mM of 2-HBP (right panels). The image shows the primary result of one representative experiment.

13 bp separation reported in other operons. This shorter distance allowed translational coupling of *dszB* and *dszC* (Martin-Cabello *et al*., 2020), not detected in other operons with longer intervals (Li *et al*., 2007).

This similarity is also extended to the *dszR* regulatory gene and the intervening genes between the structural and the regulatory *dsz* operons. However, analyses of the sequences flanking the *dsz* operons in both fosmids show that the conserved regions occupy very different genomic contexts, which suggest that the entire gene cluster was transferred laterally as a genomic island to two independent bacterial strains in separate events, a view also supported by the identification of complete and truncated *orfs* encoding for mobile elements just upstream of *dszE*. Although the recipient bacterial strains are different, they are very similar to *Candidatus* Macondimonas diazotrophica, recently described as one of the most dominant bacteria in oil-contaminated coastal sediments. Acquisition of DBT usage capacity as a sulfur source would certainly provide an important selective

Table 1. Effect of adding 2-HBP on *E coli* growth.

Conditions	% of growth
SO_4 + 0.2 mM 2-HBP	84.9 ± 6.5
SO_4 + 0.4 mM 2-HBP	66.2 ± 7.9
Taurine +0.2 mM 2-HBP	91.9 ± 9.3
Taurine +0.4 mM 2-HBP	66.4 ± 14.7
DBT + 0.2 mM 2-HBP	88.3 ± 14.6
DBT + 0.4 mM 2-HBP	66.4 ± 11.8

Growth on different sulfur sources in the presence of 2-HBP relative to growth without 2-HBP (100%).

advantage that, added to its ability to fix atmospheric nitrogen (Karthikeyan *et al*., 2019), would allow the strains to thrive successfully in these excessively carbon-rich environments.

The *dszEABC* operon in UPO112 can be expressed on its own in *E coli* and *Pseudomonas*, unlike that found in UPO21. As in previously described systems (Li *et al*., 1996; Denis-Larose *et al*., 1997; Takada *et al*., 2005; Alves *et al*., 2007; Feng *et al*., 2016; Murarka *et al*., 2019; Murarka and Srivastava, 2019), its

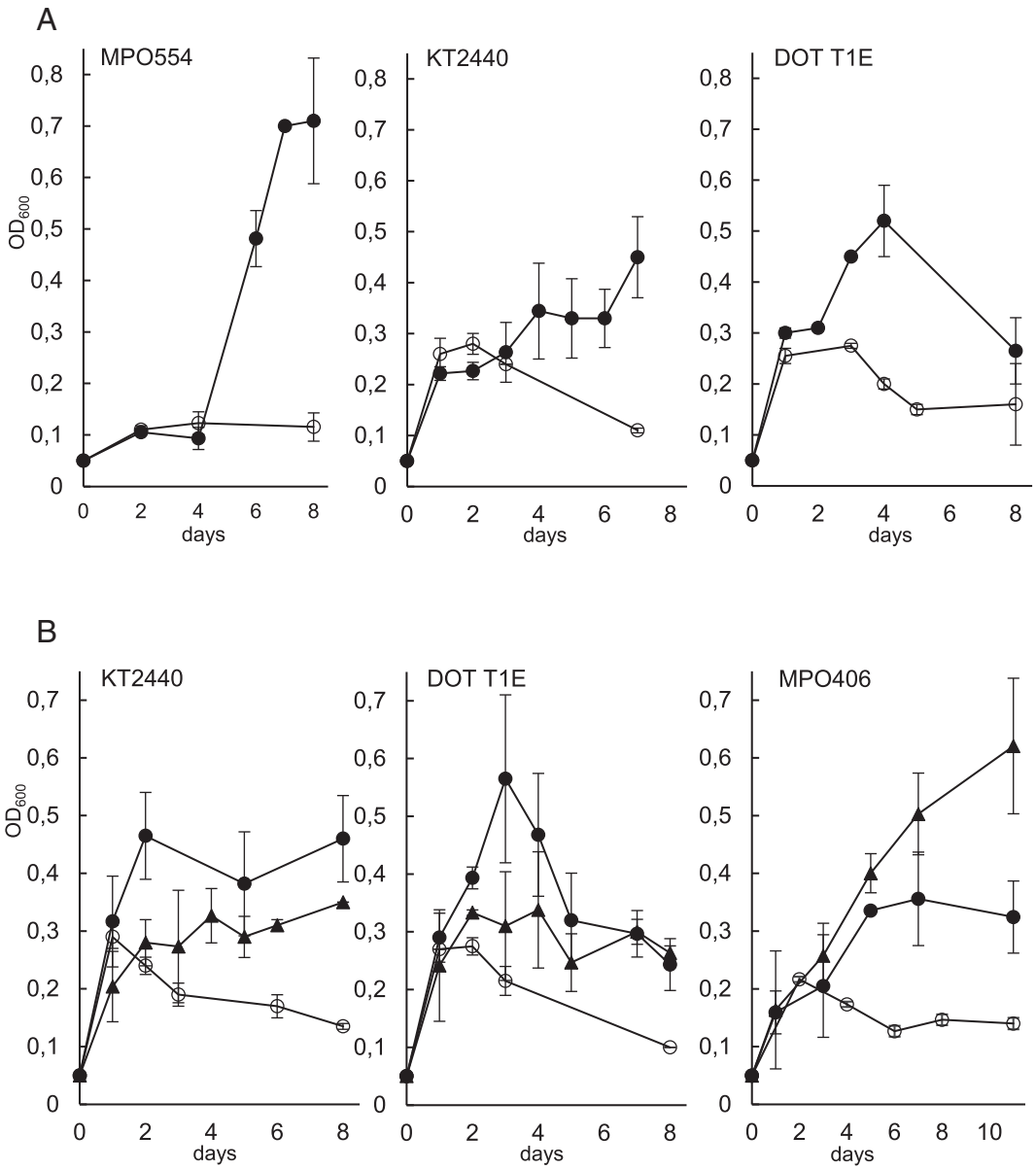

Fig. 10. Growth or different strains in minimal medium with DBT 0.2 mM as the only sulfur source.
A. MPO554 NalR, KT2440 and DOT T1E with pMPO1566 (filled circles) or the empty plasmid pSEVA221 (empty circles).
B. KT2440, DOT T1E and MPO406 with pMPO1570, with DCPK (triangles) or without DCPK (filled circles) as inducer, or the empty plasmid pSEVA429, with addition of DCPK (empty circles). In both panels, values are the average of at least three independent replicates; error bars represent standard errors.

Table 2. 2-HBP production after growth in minimal medium to stationary phase.

Strain	DCPK	Sulfur source	2-HBP (mM)
MPO554/pMPO1566	–	DBT	0.053 ± 0.006
KT2440/pMPO1566	–	DBT	0.101 ± 0.005
KT2440/pMPO1566	–	DBT + SO_4	0.004 ± 0.001
DOT T1E/pMPO1566	–	DBT	0.139 ± 0.026
DOT T1E/pMPO1566	–	DBT + SO_4	0.004 ± 0.003
KT2440/pMPO1570	–	DBT	0.114 ± 0.027
KT2440/pMPO1570	–	DBT + SO_4	0.036 ± 0.002
KT2440/pMPO1570	+	DBT	0.082 ± 0.008
KT2440/pMPO1570	+	DBT + SO_4	0.014 ± 0.002
DOT T1E/pMPO1570	–	DBT	0.133 ± 0.030
DOT T1E/pMPO1570	–	DBT + SO_4	0.036 ± 0.006
DOT T1E/pMPO1570	+	DBT	0.088 ± 0.017
DOT T1E/pMPO1570	+	DBT + SO_4	0.014 ± 0.003
MPO406/pMPO1570	–	DBT	0.129 ± 0.034
MPO406/pMPO1570	–	DBT + SO_4	0.042 ± 0.004
MPO406/pMPO1570	+	DBT	0.104 ± 0.024
MPO406/pMPO1570	+	DBT + SO_4	0.042 ± 0.005

Values are the average of at least three independent replicates. Values of DBT production with the empty plasmid are undetectable and are not shown for clarity.

expression is regulated by the sulfur source, while being repressed by sulfates, although the regulatory circuit is different from that previously characterized in *Gordonia*. *dszEABC* gene expression in UPO112, like in UPO21 (Martin-Cabello *et al*., 2020), is strictly dependent on DszR, an activator of σ^N-dependent promoters that lacks the N-terminal regulatory domain. This type of activators, which belong to type IV of sigma-54 dependent activators, are constitutively active, their activities being modulated by other proteins that bind to the activators themselves (Bush and Dixon, 2012). Expression of *dszR* itself is repressed by sulfate (Fig. 6B), while expression of *dszE::lacZ* is constitutive, independently of the sulfur source, when DszR is ectopically produced from a heterologous promoter (Fig. 8). Therefore, we propose a model in which transcriptional regulation of *dszEABC* by the sulfur source relies on the control of *dszR* transcription also in response to the sulfur source. Since *dszEABC* is expressed in both *E. coli* and *Pseudomonas* in a regulated manner (Fig. 6; Table 1) and the LysR-type activator CysB is described as the common master regulator in both bacterial genera, we propose that CysB is an activator of *dszR* transcription. According to this model, the sulfur limitation signal is sensed and the response is generated through the activity of CysB only.

The proposed regulation model is then similar to that described for biodegradation of aliphatic sulfonates in *Pseudomonas*, which involves the participation of SfnR, the activator of σ^N-dependent promoters, which as DszR also lacks the N-terminal regulatory domain, and whose expression is regulated by sulfur (Endoh *et al*., 2003a; Kouzuma *et al*., 2008). This regulatory similarity together with the similarity of DszE to the SsuE electron donors involved in degradation of aliphatic sulfonates (Fig. 3C) made us suggest that both the electron donor and the regulator might have been recruited from the same source in the same evolutionary event (Martin-Cabello *et al*., 2020). However, the fact that a very similar structural *dszEABC* operon has been found in the genome of *Comamonadaceae bacterium*, which lacks *dszR*, indicates that the regulatory circuit might have been acquired independently of *dszE*, as is apparently usual for structural and regulatory genes in many biodegradation pathways (Cases and de Lorenzo, 2001). This regulatory system suggests that the specific activator may have been easily recruited from other organosulfurated utilization systems without the need to evolve to fit its new target operon, simply by also recruiting a sulfur-regulatable target promoter region to the *dszEABC* operon.

The role of *dszH* (where the H stands for Helper) in the expression of *dszEABC* is somehow intriguing. On the one hand, two different internal in frame deletions had a severe effect on *dszEABC* expression when *dszHR* was transcribed from its own promoter (Fig. 7C), or from the basal level of the P_{tac} promoter (Fig. 8), indicating that the *orf* encoding DszH is important for *dszEABC* expression, although not involved in sensing or responding to sulfur limitation. However, this defect could not be complemented by a copy of *dszH* ectopically transcribed from the P_{tac} promoter (Fig. 7D), indicating that its function cannot be provided *in trans*. As transcription of *dszH* is not substantially diminished by the largest *dszH* internal deletions (Fig. 7E), the deletions should have a *cis* effect on translation of *dszH*. This rules out the possibility that DszR required the action of DszH to become active, a view also in contradiction with the fact that *dszR* can activate *dszEABC* expression in the absence of *dszH* if transcribed to sufficiently high levels (Fig. 8), or by the *in vitro* activity of purified $DszR_{UPO21}$ (Martin-Cabello *et al*., 2020). It is possible that deletions remove an RNA binding site required for a protein to activate *dszR* translation. Since isolated *dsz* genes can be expressed by themselves in both *E. coli* and *Pseudomonas* (Figs 7A, 8 and 10A), the genomes of both bacteria, none of which biodegrade DBT, would have to encode for this unknown activator, which is unlikely. The putative translation activator could be DszH itself. The deletions would then destroy both the translation activation function of DszH and its RNA binding site, which would be located within its own coding sequence. Although this possibility cannot be formally ruled out, we think it is unlikely since the only known domain identified in DszH is a serine hydrolase domain that covers most of the protein sequence.

We rather favour the view that *dszR* translation is enhanced by *dszH* translation *per se*. Translational coupling is a phenomenon observed in many bacterial and archaeal operons by which translation of a downstream

cistron requires prior translation of the preceding, closely located, or even overlapping, cistron of the operon (Huber *et al*., 2019). However, as the internal deletions generated in *dszH* were in frame, translation of the deleted *dszH* cistrons would terminate at exactly the same position, although generating a shorter DszH peptide. The importance of the preceding *orf* sequence on the efficiency of translational coupling has not been studied in detail, but there are other instances demonstrating the importance of translating internal sequences of the proximal cistron for efficient translational coupling of the distal cistron (Little *et al*., 1989), probably because these sequences are involved in formation of pseudoknots (Asano *et al*., 1991), or alternative secondary structures (Rex *et al*., 1994) that keep the distal cistron's ribosome binding site in an 'open' conformation state that favours its translation.

The Dsz proteins encoded in UPO112 were also able to degrade 4,6-DMDBT (Fig. 2). These were expressed independently in different genomic backgrounds (Figs 1 and 10), and their function was not strongly inhibited by 2-HBP; these characteristics make them excellent candidates for DBT degradation biocatalyst development. Since development of a viable BDS process depends on many different factors, we constructed two mobilizable broad host range biocatalysts to be used in other Gram-negative strains that may have other characteristics of interest for BDS processes (Martinez *et al*., 2016), such as biofilm overproduction (Dorado-Morales *et al*., 2021), solvent (Tao *et al*., 2011) or 2-HBP tolerance (Garcia *et al*., 2014), among others. The UPO112 Dsz genes were functional in *Pseudomonas* strains, both under their own promoter and regulatory elements, and from heterologous expression systems (Fig. 10). Expression on their own might have some limitations, such as sulfate repression or lack of positive controls regulating *dsz* genes in another bacterial host. We do not anticipate this to be a significant problem, as CysB appears to be a conserved master regulator of sulfur metabolism among several classes of proteobacteria, in addition to enterobacteria and *Pseudomonas* (Lochowska *et al*., 2011; Feng *et al*., 2021). In addition, we envisage that there should not be much sulfate available to repress *dsz* genes in a BDS process downstream of hydrodesulfurization. Nevertheless, the use of the ectopic expression vectors could complement the other biocatalyst if not active in particular backgrounds. In this case, at least in *Pseudomonas*, it appears that the high basal expression from P_{alkB} is enough to support full growth on DBT, thus preventing the need of inducers in the BDS process.

Finally, these biocatalysts could potentially be used for alternative applications such as production of high-value products (Kilbane 2nd, 2006; Kilbane 2nd and Stark, 2016).

Experimental procedures

Bacteria and growth conditions

Bacterial strains used in this work, together with their more relevant features, are summarized in Supporting Table S3.

The rich medium used was LB (Sambrook and Maniatis, 2000). The minimal medium used for *E. coli* strains was adapted M9 as previously described (Martin-Cabello *et al*., 2020), supplemented with magnesium sulfate, taurine (2-aminoethanesulfonic acid), DBT or 4,6-DMDBT 0.2–1 mM (in N,N-dimethylformamide) as the sulfur source. For the experiments in nitrogen limitation, the M9 medium was prepared without ammonium chloride, and 1 mM of L-glutamine or L-arginine, or 18.7 mM of ammonium chloride, were subsequently added as nitrogen sources. For *Pseudomonas* strains the minimal medium used for toxicity assay was a modification of a previously described minimal medium (Mandelbaum *et al*., 1993), containing 20 mM sodium succinate as carbon source and ammonium chloride (1 g L^{-1}) as nitrogen source. For growth curves with 0.2 mM of DBT as the sole sulfur source, the minimal medium used was a modification of M9 with the trace solution (Abril *et al*., 1989), supplemented with 0.1 mM calcium chloride and 20 mM sodium succinate as carbon source, to which 1/1000× of a 0.2 M DBT stock solution in N,N-dimethylformamide was added.

For monitoring growth in different sulfur sources, or determining expression of *dszE::lacZ* after growing in different sulfur or nitrogen sources, preinocula were made in LB medium. After saturation, strains were diluted at OD_{600} 0.1 in their corresponding minimal medium with sulfate 0.2 mM as sulfur source and incubated for 24 h. For *E. coli*, the cultures were then washed three times, and diluted to DO_{600} 0.05–0.1 in fresh minimal medium with the required sulfur or nitrogen source. In the case of *Pseudomonas*, cells were washed after growth in sulfate, inoculated in fresh minimal medium without sulfur source, and incubated O/N, to consume as much as possible the sulfur accumulated by the cells. Finally, bacteria were diluted to DO_{600} 0.05 in fresh minimal medium with the corresponding sulfur source.

Bacteria were grown in tubes or flasks with shaking (180 r.p.m.) at 30°C, except for *E. coli* on LB, which was incubated at 37°C.

When required, the following antibiotics and other additives were used (in μg ml^{-1}): ampicillin (Ap) 100; chloramphenicol (Cm) 12.5; gentamicin (Gm) 10; nalidixic acid (Nal) 15; streptomycin (50) arabinose 1 mM, salicylate 1 mM, IPTG 1 mM, 2-HBP (0.2–0.6 mM in N,N-dimethylformamide) and DCPK 0.05% vol./vol.. The reagents were acquired from Sigma-Aldrich.

Oligonucleotides and plasmids construction

Supplementary Tables S4 and S5 describe the plasmids and oligonucleotides used in this work respectively.

DNA manipulations were performed according to standard protocols (Sambrook and Maniatis, 2000). For DNA preparations, Macherey-Nagel extraction kit was used following the manufacturer's specifications. In all plasmid construction involving PCR amplification, the polymerase used was Q5 (New England Biolabs) and reactions were performed according to the manufacturer's instructions. All newly generated plasmids were sequenced using a commercial sequencing service (Stab Vida, Caparica, Portugal).

A *dszE*$_{UPO112}$*::lacZ* transcriptional fusion (pMPO1550) was constructed by PCR-amplifying a 564 bp fragment comprising the 5′ end of *dszE*. For this, we used oligonucleotide pair dszEUPO112Fw/dszEUPO112Rv (tm: 60°C), and UPO112 as a template. The amplified fragment was digested with StuI and ligated into pMPO234, which had been previously digested with XmaI and blunt ended with Klenow. Correct cloning orientation was checked by restriction analyses.

pMPO1552 carries a 2044 bp fragment containing *dszHR* and 225 bp upstream *dszH*, which was PCR amplified using the oligonucleotide pair dszSR-112Fw2/dszSR-112Rv (tm: 62°C), and UPO112 as the template, digested with PmlI and HindIII and cloned into pMPO579 digested with the same restriction enzymes.

For pMPO1553 construction, the 2047 bp PmlI-HindIII fragment of pMPO1552, containing dsz*HR* and 224 bp upstream, was blunt-ended with Klenow and subcloned cloned into pIZ1016 previously digested with SmaI. Restriction analyses were performed to select one candidate with the fragment cloned in the same direction of the P_{tac} promoter.

To build pMPO1559, a 1.83 kbp fragment containing *dszHR* but lacking its promoter was obtained by PCR amplification with oligonucleotide pair delPdszSSalFw and dszSR-112 Rv (tm: 62°C), using pMPO1553 as template, digested with SalI and HindIII, and then ligated into pIZ1016 digested with the same restriction enzymes.

Construction of the Δ*dszH*-1 internal in frame deletion covering from codon 16 to 203 (pMPO1561) was performed by PCR amplification of two fragments using pMPO1553 as template. Fragment A (288 bp) was obtained with oligonucleotide pair dszSR-112Fw2 and del dszS Rv-A (tm: 60°C), and digested with PmlI and NsiI. Fragment B (1231 bp) was obtained with oligonucleotide pair deldszSFw-B and dszSR-112Rv (tm: 60°C) and digested with NsiI and HindIII. Both fragments were ligated at the same time, into pMPO579 digested with PmlI and III.

For pMPO1563 construction (ΔP_{dsz} Δ*dszH*-2 in frame internal deletion covering from codon 21 to 197 under the P_{tac} promoter), two fragments were generated from pMPO1553 by PCR amplification. Fragment A (303 bp) was obtained with oligonucleotide pair deldszS Fw-A/deldszS Rv-A2 (tm: 60°C) and digested with SalI and NsiI. Fragment B (1249 bp) was obtained with oligonucleotide pair deldszS Fw-B2/dszSR-112 Rv (tm: 60°C) and digested with NsiI and HindIII. Both inserts were ligated at the same time, into pIZ1016 digested with SalI and HindIII.

To facilitate construction of the catabolic cassettes, pMPO1565 was previously constructed. The 6.9 kbp MluI-XhoI fragment containing *dszEABC* and 1085 bp upstream was obtained by digestion of UPO112 with MluI, XhoI and NdeI, filled-in with Klenow and cloned into pBSKII+ digested with EcoRV. pMPO1566 was constructed in two subsequent steps; first, the 5.9 kbp HindIII-XbaI fragment bearing the whole *dszEABC* operon from pMPO1565 was cloned into pSEVA221 digested with the same enzymes. Second, the 2085 bp fragment containing *dszHR* was amplified from UPO112 by PCR with oligonucleotide pair dszR_orf1 HindFw/dszR_orf1Rv (tm: 62°C), digested with HindIII and ligated into the plasmid described above, digested with the same enzyme. Candidates were analysed by restriction to confirm the right orientation.

pMPO1570 construction was performed by PCR amplification of a 4.36 kbp fragment bearing *dszEABC* from pMPO1565 with oligonucleotide pair Alk-dsz Fw/Alk-dsz Rv (tm: 64°C), subsequent digestion with HindIII and SpeI and cloning into pSEVA429 digested with the same enzymes.

For pMPO1571 construction (plasmid to complement *dszH in trans*), a 960 bp deletion of pMPO1559 removing most of *dszR* was done by digesting with EcoNI + HindIII, isolating the 6.9 kbp fragment containing just 224 bp of the 5′ end of *dszR*, blunt ended with Klenow and religated.

Functional screening

A metagenomic library from an oil-contaminated soil of a refinery in Southern Spain, previously described (Terron-Gonzalez *et al*., 2016), was transferred by triparental conjugation (Figurski and Helinski, 1979) to the MPO554Nal^R strain, with DH5α/pRK2013 as the helper strain. The mating mixture was incubated on LB-agar without antibiotics overnight at 37°C, after which was plated on minimal medium M9 with salicylate 1 mM and arabinose 1 mM, and 0.2 mM DBT as the sole sulfur source, and incubated at 30°C for 48 h, until colonies appeared. Growth on DBT was confirmed in solid and liquid media.

β-Galactosidase activity assays

Cultures were grown as described in section 'Bacteria and growth conditions', and diluted in the appropriate

minimal medium, to which arabinose, salicylate or IPTG were added when required, and incubated for 22 h. Cells were permeabilized with SDS and chloroform, and β-galactosidase assays were performed as previously described (Miller, 1972).

Measurement of mRNA levels by reverse transcription and quantitative PCR

Total RNA samples of MPO554 Nal^R harbouring different plasmids, grown to mid-exponential phase, were extracted as previously described (Garcia-Gonzalez *et al*., 2005). Samples were treated with DNase I (DNA-free kit, Ambion), and the absence of DNA was confirmed by PCR amplification, after which, RNA was purified using RNeasy purification kit (Qiagen, Germany) and their integrity was confirmed by agarose gel electrophoresis. cDNA was produced using High-Capacity cDNA Archive Kit (Applied Biosystems), with 3 μg of total RNA and random hexamers as primers to generate cDNAs, following the manufacturer's indications, and purified using QIAquick PCR purification kit (Qiagen). Quantitative PCR assays were performed as described (de Dios *et al*., 2020) using 10 ng of cDNA. As template for the calibration curve, serial dilutions of each DNA plasmid (between 25 and 0.0025 ng) were used. For *dszR* expression quantification, oligonucleotides pairs used were dszRQ Fw/dszRQ Rv, and for *dszE*, dszEQ Fw2/dszEQ Rv2.

Determination of 2-hydroxybiphenyl production

Production of 2-HBP as the end product of the DBT desulfurization was measured by Gibbs assay as previously described (Murarka *et al*., 2019). The strains were grown in their respective minimal medium with DBT or DBT plus sulfate (0.2 mM each), and with addition of DCPK to induce the expression of P_{alkB} in the case of pMPO1570, when required. For each strain, 2-HBP was determined after the time necessary to achieved stationary phase when growing on DBT. The results shown are the average of at least three independent replicas. The error bars represent the standard error.

Toxicity assay

Cultures of *E. coli* MPO554 Nal^R/UPO112 in minimal liquid medium with different sulfur sources were grown as described in section 'Bacteria and growth conditions'. At the time of diluting the cells in the appropriate fresh minimal medium, 0.2 or 0.4 mM 2-HBP was added.

A drop dilution assay was also performed to evaluate the sensitivity of *E. coli* MPO554 Nal^R, *P. putida* KT2440 and DOT T1E to 2-HBP. The viability assay was performed in the minimal medium indicated above for each strain, with 1 mM sulfate as the sulfur source. The initial cultures from which serial dilutions were performed were at DO_{600} 1. 2-HBP was added at 0.2 (not shown), 0.4 and 0.6 mM.

DNA sequencing and data analysis

UPO112 was sequenced with a Roche 454 GS FLX Ti sequencer (454 Life Sciences, Branford, CT, USA) at Lifesequencing S.L. (Valencia, Spain), and the resulting nucleotide sequences were assembled using a Newbler GS v.2.3 *de novo* assembler (Roche).

The sequences obtained were compared to those in the NCBI databases (nucleotide collection, non-redundant protein sequences and UniProtKB/Swiss-Prot) using the BLAST toolkit (Altschul *et al*., 1997), and annotated according to their similarities.

MOLE-BLAST tool (https://blast.ncbi.nlm.nih.gov/moleblast/moleblast.cgi) was used to try to identify the origin of the UPO21 sequence. The genomic insert was initially divided into 5 kb fragments and parts of these fragments subsequently separated into smaller fragments. Database of Nucleotide collection (nr/nt) was selected. For the construction of phylogenetic trees, multiple-sequence alignment was performed using MEGAX (Kumar *et al*., 2018), employing MUSCLE as the alignment method. Phylogenetic trees were estimated using the Maximum Likelihood method, choosing the best model indicated by MEGAX in each case and selecting in the Gap/Missing Data Treatment parameter the Partial Deletion option. A bootstrap analysis was run, selecting a number of bootstrap replicates of 100.

Accession number

The insert sequence in UPO112 has been submitted to the DDBJ/EMBL/GenBank/DBBJ under accession number MZ596412.

Acknowledgements

We are grateful to all members of the laboratory for their insights and helpful suggestions. This project has received funding from grants BIO2014-54494-R and BIO2017-85522-R from the Ministerio de Ciencia e Innovación.

References

Abbasian, F., Lockington, R., Megharaj, M., and Naidu, R. (2016) Identification of a new operon involved in desulfurization of dibenzothiophenes using a metagenomic study and cloning and functional analysis of the genes. *Enzyme Microb Technol* **87-88**: 24–28.

Abin-Fuentes, A., Mohamed Mel, S., Wang, D.I., and Prather, K.L. (2013) Exploring the mechanism of biocatalyst inhibition in microbial desulfurization. *Appl Environ Microbiol* **79**: 7807–7817.

Abril, M.A., Michan, C., Timmis, K.N., and Ramos, J.L. (1989) Regulator and enzyme specificities of the TOL plasmid-encoded upper pathway for degradation of aromatic hydrocarbons and expansion of the substrate range of the pathway. *J Bacteriol* **171**: 6782–6790.

Altschul, S.F., Madden, T.L., Schaffer, A.A., Zhang, J., Zhang, Z., Miller, W., and Lipman, D.J. (1997) Gapped BLAST and PSI-BLAST: a new generation of protein database search programs. *Nucleic Acids Res* **25**: 3389–3402.

Alves, L., Melo, M., Mendonca, D., Simoes, F., Matos, J., Tenreiro, R., and Girio, F. (2007) Sequencing, cloning and expression of the dsz genes required for dibenzothiophene sulfone desulfurization from Gordonia alkanivorans strain 1B. *Enzyme Microb Technol* **40**: 1598–1603.

Amador, C.I., Canosa, I., Govantes, F., and Santero, E. (2010) Lack of CbrB in Pseudomonas putida affects not only amino acids metabolism but also different stress responses and biofilm development. *Environ Microbiol* **12**: 1748–1761.

Amador, C.I., Lopez-Sanchez, A., Govantes, F., Santero, E., and Canosa, I. (2016) A Pseudomonas putida cbrB transposon insertion mutant displays a biofilm hyperproducing phenotype that is resistant to dispersal. *Environ Microbiol Rep* **8**: 622–629.

Asano, K., Kato, A., Moriwaki, H., Hama, C., Shiba, K., and Mizobuchi, K. (1991) Positive and negative regulations of plasmid CoLIb-P9 repZ gene expression at the translational level. *J Biol Chem* **266**: 3774–3781.

Brunet, S.M.D., Pérot, G., Bouchy, C., and Diehl, F. (2005) On the hydrodesulfurization of FCC gasoline: a review. *Appl Catal Gen* **278**: 29–172.

Bush, M., and Dixon, R. (2012) The role of bacterial enhancer binding proteins as specialized activators of sigma54-dependent transcription. *Microbiol Mol Biol Rev* **76**: 497–529.

Cases, I., and de Lorenzo, V. (2001) The black cat/white cat principle of signal integration in bacterial promoters. *EMBO J* **20**: 1–11.

de Dios, R., Rivas-Marin, E., Santero, E., and Reyes-Ramirez, F. (2020) Two paralogous EcfG sigma factors hierarchically orchestrate the activation of the general stress response in Sphingopyxis granuli TFA. *Sci Rep* **10**: 5177.

Denis-Larose, C., Labbe, D., Bergeron, H., Jones, A.M., Greer, C.W., al-Hawari, J., *et al*. (1997) Conservation of plasmid-encoded dibenzothiophene desulfurization genes in several rhodococci. *Appl Environ Microbiol* **63**: 2915–2919.

Denome, S.A., Oldfield, C., Nash, N.J., and Young, K.D. (1994) Characterization of the desulfurization genes from Rhodococcus sp. strain IGTS8. *J Bacteriol* **176**: 6707–6716.

Dorado-Morales, P., Martinez, I., Rivero-Buceta, V., Diaz, E., Bahre, H., Lasa, I., and Solano, C. (2021) Elevated c-di-GMP levels promote biofilm formation and biodesulfurization capacity of Rhodococcus erythropolis. *J Microbial Biotechnol* **14**: 923–937.

Endoh, T., Habe, H., Nojiri, H., Yamane, H., and Omori, T. (2005) The sigma54-dependent transcriptional activator SfnR regulates the expression of the Pseudomonas putida sfnFG operon responsible for dimethyl sulphone utilization. *Mol Microbiol* **55**: 897–911.

Endoh, T., Habe, H., Yoshida, T., Nojiri, H., and Omori, T. (2003a) A CysB-regulated and sigma54-dependent regulator, SfnR, is essential for dimethyl sulfone metabolism of Pseudomonas putida strain DS1. *Microbiology* **149**: 991–1000.

Endoh, T., Kasuga, K., Horinouchi, M., Yoshida, T., Habe, H., Nojiri, H., and Omori, T. (2003b) Characterization and identification of genes essential for dimethyl sulfide utilization in Pseudomonas putida strain DS1. *Appl Microbiol Biotechnol* **62**: 83–91.

Feng, S., Qiu, Y., Huang, Z., Yin, Y., Zhang, H., Zhu, D., *et al*. (2021) The adaptation mechanisms of Acidithiobacillus caldus CCTCC M 2018054 to extreme acid stress: bioleaching performance, physiology, and transcriptomics. *Environ Res* **199**: 111341.

Feng, S.Y.,.H., Zhan, X., and Wang, W. (2016) Enhancement of dibenzothiophene biodesulfurization via weakening feedback inhibition effects based on system-understanding of biodesulfurization mechanism by Gordonia sp. through potential "4S" pathway. *R Soc Adv* **6**: 8271–82881.

Figurski, D.H., and Helinski, D.R. (1979) Replication of an origin-containing derivative of plasmid RK2 dependent on a plasmid function provided in trans. *Proc Natl Acad Sci U S A* **76**: 1648–1652.

Furuya, T., Takahashi, S., Ishii, Y., Kino, K., and Kirimura, K. (2004) Cloning of a gene encoding flavin reductase coupling with dibenzothiophene monooxygenase through coexpression screening using indigo production as selective indication. *Biochem Biophys Res Commun* **313**: 570–575.

Furuya, T., Takahashi, S., Iwasaki, Y., Ishii, Y., Kino, K., and Kirimura, K. (2005) Gene cloning and characterization of Mycobacterium phlei flavin reductase involved in dibenzothiophene desulfurization. *J Biosci Bioeng* **99**: 577–585.

Gallardo, M.E., Ferrandez, A., De Lorenzo, V., Garcia, J.L., and Diaz, E. (1997) Designing recombinant Pseudomonas strains to enhance biodesulfurization. *J Bacteriol* **179**: 7156–7160.

Garcia, J.L., Rozas, D., Del Cerro, C., Nogales, J., El-Said Mohamed, M., and Diaz, E. (2014) Genome sequence of Pseudomonas azelaica HBP1, which catabolizes 2-hydroxybiphenyl fungicide. *Genome Announc* **2**: e01248-13.

Garcia-Gonzalez, V., Govantes, F., Porrua, O., and Santero, E. (2005) Regulation of the Pseudomonas sp. strain ADP cyanuric acid degradation operon. *J Bacteriol* **187**: 155–167.

Gray, K.A., Pogrebinsky, O.S., Mrachko, G.T., Xi, L., Monticello, D.J., and Squires, C.H. (1996) Molecular mechanisms of biocatalytic desulfurization of fossil fuels. *Nat Biotechnol* **14**: 1705–1709.

Habe, H., Kouzuma, A., Endoh, T., Omori, T., Yamane, H., and Nojiri, H. (2007) Transcriptional regulation of the

sulfate-starvation-induced gene sfnA by a sigma54-dependent activator of Pseudomonas putida. *Microbiology* **153**: 3091–3098.

Huber, M., Faure, G., Laass, S., Kolbe, E., Seitz, K., Wehrheim, C., *et al*. (2019) Translational coupling via termination-reinitiation in archaea and bacteria. *Nat Commun* **10**: 4006.

Ishii, Y., Konishi, J., Okada, H., Hirasawa, K., Onaka, T., and Suzuki, M. (2000b) Operon structure and functional analysis of the genes encoding thermophilic desulfurizing enzymes of Paenibacillus sp. A11-2. *Biochem Biophys Res Commun* **270**: 81–88.

Ishii, Y., Konishi, J., Suzuki, M., and Maruhashi, K. (2000a) Cloning and expression of the gene encoding the thermophilic NAD(P)H-FMN oxidoreductase coupling with the desulfurization enzymes from Paenibacillus sp. A11-2. *J Biosci Bioeng* **90**: 591–599.

Karthikeyan, S., Rodriguez, R.L., Heritier-Robbins, P., Kim, M., Overholt, W.A., Gaby, J.C., *et al*. (2019) "Candidatus Macondimonas diazotrophica", a novel gammaproteobacterial genus dominating crude-oil-contaminated coastal sediments. *ISME J* **13**: 2129–2134.

Kertesz, M.A. (2000) Riding the sulfur cycle--metabolism of sulfonates and sulfate esters in gram-negative bacteria. *FEMS Microbiol Rev* **24**: 135–175.

Khosravinia, S., Mahdavi, M.A., Gheshlaghi, R., Dehghani, H., and Rasekh, B. (2018) Construction and characterization of a new recombinant vector to remove sulfate repression of dsz promoter transcription in biodesulfurization of dibenzothiophene. *Front Microbiol* **9**: 1578.

Kilbane, J.J., 2nd. (2006) Microbial biocatalyst developments to upgrade fossil fuels. *Curr Opin Biotechnol* **17**: 305–314.

Kilbane, J.J., 2nd, and Robbins, J. (2007) Characterization of the dszABC genes of Gordonia amicalis F.5.25.8 and identification of conserved protein and DNA sequences. *Appl Microbiol Biotechnol* **75**: 843–851.

Kilbane, J.J., 2nd, and Stark, B. (2016) Biodesulfurization: a model system for microbial physiology research. *World J Microbiol Biotechnol* **32**: 137.

Kilbane, J.J., II. (2016) Biodesulfurization: how to make it work? *Arab J Sci Eng* **42**: 1–9.

Kouzuma, A., Endoh, T., Omori, T., Nojiri, H., Yamane, H., and Habe, H. (2008) Transcription factors CysB and SfnR constitute the hierarchical regulatory system for the sulfate starvation response in Pseudomonas putida. *J Bacteriol* **190**: 4521–4531.

Kumar, S., Stecher, G., Li, M., Knyaz, C., and Tamura, K. (2018) MEGA X: molecular evolutionary genetics analysis across computing platforms. *Mol Biol Evol* **35**: 1547–1549.

Li, G.Q., Ma, T., Li, S.S., Li, H., Liang, F.L., and Liu, R.L. (2007) Improvement of dibenzothiophene desulfurization activity by removing the gene overlap in the dsz operon. *Biosci Biotechnol Biochem* **71**: 849–854.

Li, L., Liao, Y., Luo, Y., Zhang, G., Liao, X., Zhang, W., *et al*. (2019) Improved efficiency of the desulfurization of oil sulfur compounds in Escherichia coli using a combination of desensitization engineering and DszC overexpression. *ACS Synth Biol* **8**: 1441–1451.

Li, M.Z., Squires, C.H., Monticello, D.J., and Childs, J.D. (1996) Genetic analysis of the dsz promoter and associated regulatory regions of Rhodococcus erythropolis IGTS8. *J Bacteriol* **178**: 6409–6418.

Little, S., Hyde, S., Campbell, C.J., Lilley, R.J., and Robinson, M.K. (1989) Translational coupling in the threonine operon of Escherichia coli K-12. *J Bacteriol* **171**: 3518–3522.

Lochowska, A., Iwanicka-Nowicka, R., Zielak, A., Modelewska, A., Thomas, M.S., and Hryniewicz, M.M. (2011) Regulation of sulfur assimilation pathways in Burkholderia cenocepacia through control of genes by the SsuR transcription factor. *J Bacteriol* **193**: 1843–1853.

Lundgren, B.R., Sarwar, Z., Feldman, K.S., Shoytush, J.M., and Nomura, C.T. (2019) SfnR2 regulates dimethyl sulfide-related utilization in Pseudomonas aeruginosa PAO1. *J Bacteriol* **201**: e00606-18.

Mandelbaum, R.T., Wackett, L.P., and Allan, D.L. (1993) Mineralization of the s-triazine ring of atrazine by stable bacterial mixed cultures. *Appl Environ Microbiol* **59**: 1695–1701.

Martin-Cabello, G., Terron-Gonzalez, L., Ferrer, M., and Santero, E. (2020) Identification of a complete dibenzothiophene biodesulfurization operon and its regulator by functional metagenomics. *Environ Microbiol* **22**: 91–106.

Martinez, I., El-Said Mohamed, M., Santos, V.E., Garcia, J. L., Garcia-Ochoa, F., and Diaz, E. (2017) Metabolic and process engineering for biodesulfurization in Gram-negative bacteria. *J Biotechnol* **262**: 47–55.

Martinez, I., Mohamed Mel, S., Rozas, D., Garcia, J.L., and Diaz, E. (2016) Engineering synthetic bacterial consortia for enhanced desulfurization and revalorization of oil sulfur compounds. *Metab Eng* **35**: 46–54.

Miller, J.H. (1972) *Experiments in Molecular Genetics*. Cold Spring Harbor, NY: Cold Spring Harbor Laboratory Press.

Mohebali, G., and Ball, A. (2016) Biodesulfurization of diesel fuels e past, present and future perspectives. *Int Biodeterior Biodegrad* **110**: 18–180.

Murarka, P., Bagga, T., Singh, P., Rangra, S., and Srivastava, P. (2019) Isolation and identification of a TetR family protein that regulates the biodesulfurization operon. *AMB Express* **9**: 71.

Murarka, P., Keshav, A., Meena, B.K., and Srivastava, P. (2020) Functional characterization of the transcription regulator WhiB1 from Gordonia sp. IITR100. *Microbiology (Reading)* **166**: 1181–1190.

Murarka, P., and Srivastava, P. (2019) Characterization of DNA binding and ligand binding properties of the TetR family protein involved in regulation of dsz operon in Gordonia sp. IITR100. *Int J Biol Macromol* **141**: 671–679.

Parveen, S., Akhtar, N., Ghauri, M.A., and Akhtar, K. (2020) Conventional genetic manipulation of desulfurizing bacteria and prospects of using CRISPR-Cas systems for enhanced desulfurization activity. *Crit Rev Microbiol* **46**: 300–320.

Piddington, C.S., Kovacevich, B.R., and Rambosek, J. (1995) Sequence and molecular characterization of a DNA region encoding the dibenzothiophene desulfurization operon of Rhodococcus sp. strain IGTS8. *Appl Environ Microbiol* **61**: 468–475.

Rex, G., Surin, B., Besse, G., Schneppe, B., and McCarthy, J.E. (1994) The mechanism of translational

coupling in Escherichia coli. Higher order structure in the atpHA mRNA acts as a conformational switch regulating the access of de novo initiating ribosomes. *J Biol Chem* **269**: 18118–18127.

Sambrook, J.F., Fritsch, E.F., and Maniatis, T. (2000) *Molecular Cloning: A Laboratory Manual*. Cold Spring Harbor, NY: Cold Spring Harbor Laboratory Press.

Sekowska, A., Kung, H.F., and Danchin, A. (2000) Sulfur metabolism in Escherichia coli and related bacteria: facts and fiction. *J Mol Microbiol Biotechnol* **2**: 145–177.

Shavandi, M., Sadeghizadeh, M., Khajeh, K., Mohebali, G., and Zomorodipour, A. (2010) Genomic structure and promoter analysis of the dsz operon for dibenzothiophene biodesulfurization from Gordonia alkanivorans RIPI90A. *Appl Microbiol Biotechnol* **87**: 1455–1461.

Silva-Rocha, R., Martinez-Garcia, E., Calles, B., Chavarria, M., Arce-Rodriguez, A., de Las Heras, A., *et al*. (2013) The Standard European Vector Architecture (SEVA): a coherent platform for the analysis and deployment of complex prokaryotic phenotypes. *Nucleic Acids Res* **41**: D666–D675.

Stec, E., Witkowska-Zimny, M., Hryniewicz, M.M., Neumann, P., Wilkinson, A.J., Brzozowski, A.M., *et al*. (2006) Structural basis of the sulphate starvation response in E. coli: crystal structure and mutational analysis of the cofactor-binding domain of the Cbl transcriptional regulator. *J Mol Biol* **364**: 309–322.

Takada, M., Nomura, N., Okada, H., Nakajima-Kambe, T., Nakahara, T., and Uchiyama, H. (2005) De-repression and comparison of oil-water separation activity of the dibenzothiophene desulfurizing bacterium, Mycobacterium sp. G3. *Biotechnol Lett* **27**: 871–874.

Tanaka, Y., Yoshikawa, O., Maruhashi, K., and Kurane, R. (2002) The cbs mutant strain of Rhodococcus erythropolis KA2-5-1 expresses high levels of Dsz enzymes in the presence of sulfate. *Arch Microbiol* **178**: 351–357.

Tao, F., Liu, Y., Luo, Q., Su, F., Xu, Y., Li, F., *et al*. (2011) Novel organic solvent-responsive expression vectors for biocatalysis: application for development of an organic solvent-tolerant biodesulfurizing strain. *Bioresour Technol* **102**: 9380–9387.

Terron-Gonzalez, L., Martin-Cabello, G., Ferrer, M., and Santero, E. (2016) Functional metagenomics of a biostimulated petroleum-contaminated soil reveals an extraordinary diversity of extradiol dioxygenases. *Appl Environ Microbiol* **82**: 2467–2478.

Terron-Gonzalez, L., Medina, C., Limon-Mortes, M.C., and Santero, E. (2013) Heterologous viral expression systems in fosmid vectors increase the functional analysis potential of metagenomic libraries. *Sci Rep* **3**: 1107.

Thompson, D., Cognat, V., Goodfellow, M., Koechler, S., Heintz, D., Carapito, C., *et al*. (2020) Phylogenomic classification and biosynthetic potential of the fossil fuel-biodesulfurizing Rhodococcus strain IGTS8. *Front Microbiol* **11**: 1417.

van der Ploeg, J.R., Eichhorn, E., and Leisinger, T. (2001) Sulfonate-sulfur metabolism and its regulation in Escherichia coli. *Arch Microbiol* **176**: 1–8.

van der Ploeg, J.R., Iwanicka-Nowicka, R., Kertesz, M.A., Leisinger, T., and Hryniewicz, M.M. (1997) Involvement of CysB and Cbl regulatory proteins in expression of the tauABCD operon and other sulfate starvation-inducible genes in Escherichia coli. *J Bacteriol* **179**: 7671–7678.

Vilchez-Vargas, R., Junca, H., and Pieper, D.H. (2010) Metabolic networks, microbial ecology and 'omics' technologies: towards understanding in situ biodegradation processes. *Environ Microbiol* **12**: 3089–3104.

Wang, J., Butler, R.R., 3rd, Wu, F., Pombert, J.F., Kilbane, J.J., 2nd, and Stark, B.C. (2017) Enhancement of microbial biodesulfurization via genetic engineering and adaptive evolution. *PLoS One* **12**: e0168833.

Supporting Information

Additional Supporting Information may be found in the online version of this article at the publisher's web-site:

Appendix S1: Supplementary Information